Available online at www.eccomasproceedia.org
Eccomas Proceedia SMART (2023) 899-910

ECCOMAS
Proceedia

X ECCOMAS Thematic Conference on Smart Structures and Materials
SMART 2023
D.A. Saravanos, A. Benjeddou, N. Chrysochoidis and T. Theodosiou (Eds)

DIGITAL TWIN-BASED DAMAGE QUANTIFICATION ON COMPOSITE STRUCTURES

Dimitrios Milanoski[1], Georgios Galanopoulos[1], Dimitrios Zarouchas[2] and Theodoros Loutas[1]

[1]Laboratory of Applied Mechanics and Vibrations
Department of Mechanical Engineering and Aeronautics
University of Patras, 26504 Rio, Greece
e-mail: thloutas@upatras.gr

[2] Center of Excellence in Artificial Intelligence for Structures, Prognostics & Health Management
Faculty of Aerospace Engineering
Delft University of Technology, Delft, The Netherlands
e-mail: D.Zarouchas@tudelft.nl

Abstract. In the present study a digital twin-based methodology for Structural Health Monitoring (SHM) of composite stiffened panels is developed. More specifically, beyond damage detection and localization, the quantification of damage is determined based on relevant damaged training data provided by a numerical campaign. Parametric finite element models with distinct damage morphologies, i.e. skin-to-stringer delaminations, are generated based on a Latin hypercube sampling plan. The above sampling plan generates an adequate amount of simulated strain data capable of establishing a relation among the damage characteristics, i.e. damage size and location, and the longitudinal strain at specific sensing locations. Hence, Gaussian process (GP) surrogate models are trained with the numerically generated data and their hyperparameters are determined via Bayesian optimization. The damage quantification is treated as a minimization problem, the solution of which is obtained via a global optimization iterative procedure. The methodology is assessed utilizing a single-stringer composite panel with a rectangle skin/stringer artificial delamination. Compressive loads are applied on the panel and longitudinal static strains are received by permanently fiber Bragg grating sensors affixed onto the stringer feet. The pre-trained GP models are fed with experimental strains during testing and in turn yield the damage characteristics of the delamination. The methodology is also applicable to unknown load conditions as it predicts the load acting on the panel on the first SHM levels. Promising results are obtained, empowering the viewpoint of the proposed methodology which aims to harness the contemporary capabilities of numerical models toward real-time damage diagnosis on complicated structures.

Key words: Structural Health Monitoring, Digital twin, Composite stiffened panels, Surrogate modeling

Peer-review under responsibility of the organizing committee of SMART 2023.
doi: 10.7712/150123.9842.445107

1 INTRODUCTION

Over the last decade the prominent *digital twin* (DT) concept emerges rapidly, and intensive research around this topic is being developed. The concept is adapted by a vast range of engineering areas, e.g. manufacturing, mechanical, aerospace, civil, energy and other [1, 2, 3]. A comprehensive review paper has been recently published which encompasses the wide range of twinning enabling technologies [4]. The origins of the DT are found in the aerospace section where initially the term was introduced [5, 6]. Concretely, the DT may be defined as a digital replica of a physical asset that is capable of mimicking the behavior of the latter, based on real-time data received by the physical counterpart. The role of the DT is to mirror the response of the physical asset relying on uninformative data received during operational conditions. Having readily available a DT enables great benefits which are related to aspects such as product development, performance and health monitoring of the physical asset or predictive capabilities, e.g. remaining useful life estimation.

Advanced numerical modeling provides a favorable solution in DT development, as complicated systems/structures can be numerically analyzed, e.g. finite element (FE) analysis, in cases that analytical solutions are painful to derive. For example, modern aerospace structures are characterized by their complicated nature of damage development under operational conditions, especially for composite materials. These structures are profoundly known for the damage-tolerant capabilities they are providing [7]. However, it is of paramount importance to early detect and monitor the propagation of crucial structural damage in critical areas of the structure in order to avoid sudden failure. The DT may assist the critical tasks of Structural Health Monitoring (SHM) which are further subdivided into (1) diagnostics and (2) prognostics. Diagnostics tasks are determined to detect, localize and quantify damage [8], whilst prognostics are designated to estimate the remaining useful life [9, 10].

Machine learning techniques are utilized to alleviate extensive numerical campaigns by offering great interpolation opportunities via surrogate models [11]. A common approach to acquire training data for the surrogate models is by directly receiving experimental measurements from the subject physical asset while operating [12]. On the other hand, leveraging on numerical models to produce the relevant training data is an alternative; numerical models are used to generate the training dataset of the surrogate models that would be utilized to perform SHM strategies [13, 14]. The data generation and training of the surrogates are frequently conducted offline whilst the diagnostic actions are being implemented during the online stage. The DT concept via surrogate modeling is based on the idea to utilize the trained surrogate model(s) and perform diagnostic actions during operation by constantly receiving data from the physical counterpart [15, 16]. A variety of methodologies on DT-based damage quantification can be find in the literature, distinguished among each other depending on the nature of the measured data, e.g. strains [17], guided waves [18], acoustic emission [19] etc., the type of surrogate models or the damaged dataset source.

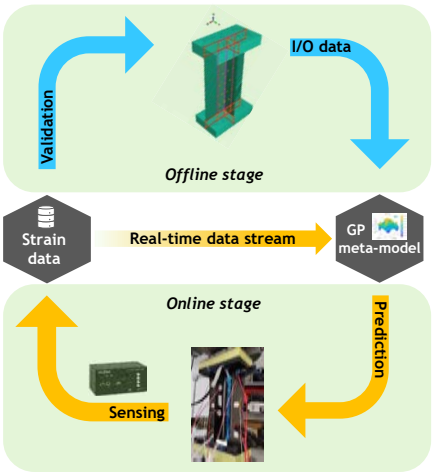

Figure 1: Digital twin concept

2 METHODOLOGY OUTLOOK

The concept herein relies on the quantification of typical skin-to-stringer disbonds existing at composite stiffened panels. The disbond area and location are estimated by utilizing real-time experimental strains placed along the stringer feet. To achieve this, a validated parametric FE model is utilized to generate relevant disbond morphologies out of which strains are estimated at the corresponding locations where the strain sensors are placed. The generated simulated strains are then used to train surrogate Gaussian Process models (GPs) in order to establish a relation among the disbond characteristics, i.e. disbond location and length, with the axial strains at the sensing locations. Then, an inverse estimation is of the disbond characteristics is followed via a global optimization procedure.

The DT concept is thus divided into two stages, as shown in Figure 1; the offline stage during which the parametric FE model generates a strain databank that will be training the surrogate models. The offline stage will constitute the digital counterpart of the physical stiffened panel which will be feeding strains, during the online stage, to the optimization scheme in order to quantify the disbond area and location. The methodology also takes into account the variability on the compressive load applied to the panel by performing load identification prior to the disbond quantification [20, 21].

3 DIGITAL TWIN DEVELOPMENT

3.1 Parametric finite element model

The numerical campaign is designed utilizing a previously developed and validated FE model of a single-stringer panel (SSP) subject to quasi-static compressive loads [22]. The SSP operates both on a linear as well as a nonlinear post-buckling regime. The panel consists of a flat composite skin co-bonded with a T-stringer in the middle area of the skin. At both ends, the SSP is encased within epoxy cast-tabs to facilitate the load introduction. The details of the composite

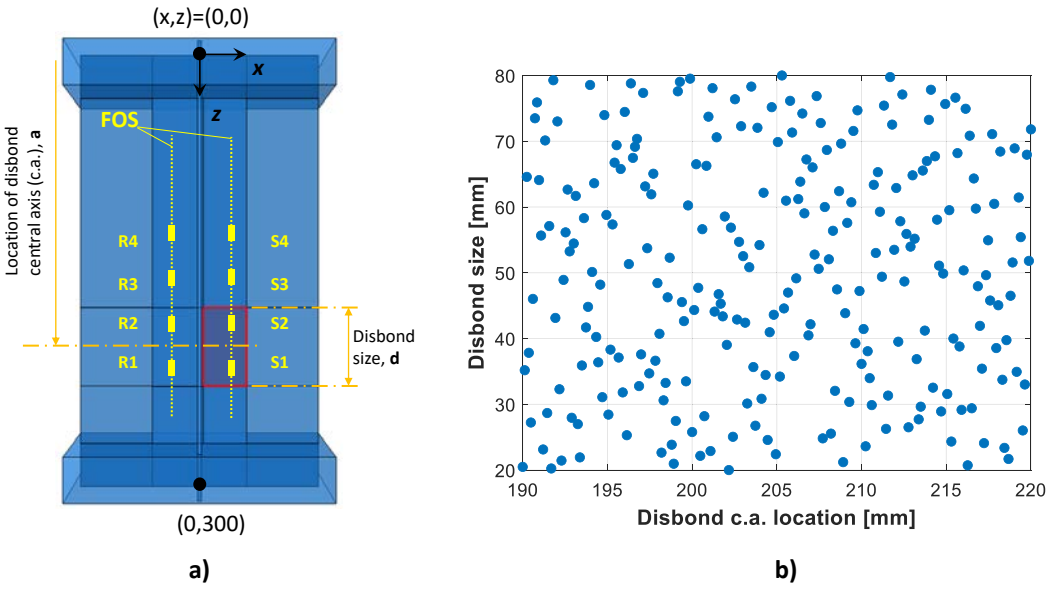

Figure 2: a) Parametric FE model with sensing locations and b) LH sampling plan

SSP, such as stacking sequence and material properties, are provided in section "Experimental Evaluation".

Commercial FE package ABAQUS/CAE 2021™ was used to perform the nonlinear static analysis. The bonded cross-sections between skin/stringer/cast-tabs are connected using tie constraints. Continuum shell elements with reduced integration (SC8R) were selected for the composite parts whereas the cast tabs were discretized with three-dimensional brick elements with reduced integration scheme (C3D8R). Displacement-control boundary conditions are applied in the SSP, with the bottom surface of the cast-tab having all its degrees of freedom fixed whilst the nodes of the top cast-tab surface have only the longitudinal displacement degree of freedom unrestricted. The strains derive after performing a two-step analysis to obtain the solution. The first part consists of linear (perturbation) buckling analysis which assists the imminent nonlinear buckling analysis utilizing Newton-Raphson solver with large displacement formulation enabled.

Discrete disbond morphologies are created to generate the training data for the surrogate models. Rectangle disbonds placed amidst the skin/stringer surface are developed by eliminating the kinematic restrictions among the kissing nodes of the skin/stringer surface. The two main parameters of the disbonds are depicted in Figure 2, i.e. the location of the disbond central axis (a) and the disbond size (d) along the longitudinal directions. In our study, the width of the disbond is maintained constant, relying on the observation that skin/stringer interfacial disbonds are mainly propagating along the longitudinal direction. This assumption allows the reduction of design space dimensionality and alleviates the numerical campaign from further computational burden. The disbond morphologies are defined by a Latin Hypercube (LH) sam-

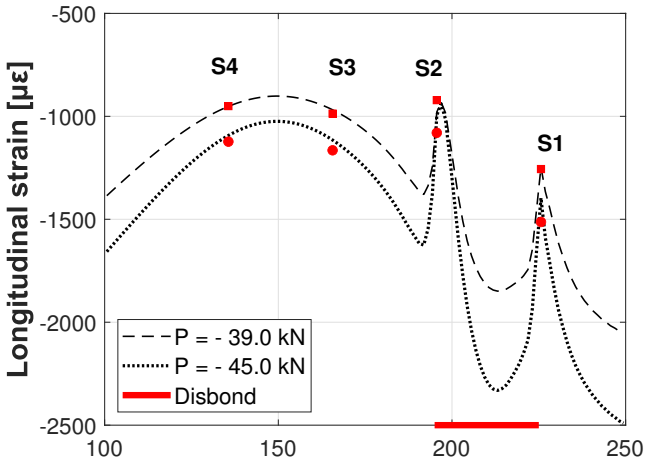

Figure 3: Simulated strain distribution along longitudinal direction with the presence of a 30x30 mm^2 disbond. Solid red square and circle markers indicate experimental strains from a damaged panel [21]

pling plan, as shown in Figure 2b, to endow space-filling capabilities to the training points and reduce the curse of dimensionality phenomenon. In total, 250 models have been constructed with $a \in [190, 220]$ and $d \in [20, 80]$ with respect to the coordinate system in Figure 2a. The parametric FE model was developed utilizing *Python*™ scripting to amend the disbond parameters according to the sampling plan.

3.2 Damaged strain data generation

The presence of skin/stringer delamination is captured by acquiring strain data from the sensing points S1-S4. Each disbond morphology develops a specific strain signature, as presented in Figure 3, which is also affected by the load magnitude (P) [23, 24]. As far there is an sufficient amount of data to associate the disbond parameters with the output strain , as estimated by the FE analysis, we will be able to construct substitute surrogate models, $\widetilde{\mathcal{M}}_{S_i}$, that would be deriving the longitudinal strain at each sensing location based on the provided input, i.e. a, d, P.

3.3 Surrogate modeling

The DT concept in enabled via utilizing surrogate models, which have been trained offline with simulated strain data received by the numerical campaign described previously. The parametric FE model pre-calculates the induced strain at i-th sensing locations:

$$\mathcal{M}_{S_i}(\boldsymbol{x}^{(k)}) = \varepsilon_{S_i}(a^{(k)}, d^{(k)}, P^{(k)}) \tag{1}$$

where k is the training data point, ε_{S_i} is the longitudinal strain at sensing location S_i and $\boldsymbol{x}$ refers to the design variables, i.e. $\boldsymbol{x} = \{a, d, P\}^\top$. As we have posed the importance of the load to the strain field, for each disbond set, (a, d), the FE model estimates the strain output at

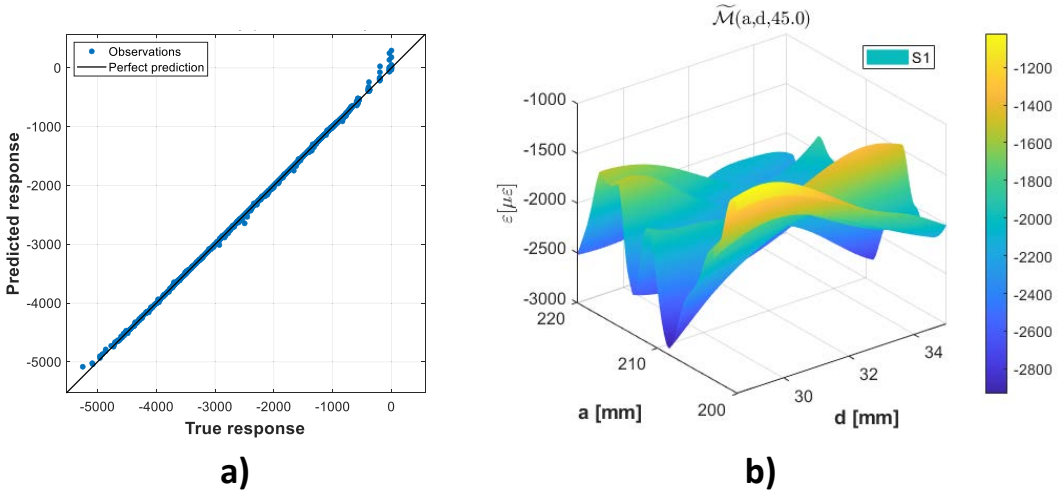

Figure 4: a) Predicted vs. actual strains of the trained $\widetilde{\mathcal{M}}_{S_1}$ and b) response surface of the surrogate under compressive load $P = -45.0$ kN

different load levels, uniformly distributed in a range of $[0, 70]$ kN, $P \sim \mathcal{U}(0, 70)$. Finally, an input/output (I/O) dataset, containing N_t I/O pairs, is constructed per sensing location S_i:

$$\mathcal{D}_{S_i} = \{\boldsymbol{x}^{(k)}; \mathcal{M}_{S_i}^{(k)}\}_{k=1}^{N_T} \tag{2}$$

The above training datasets are selected to train surrogate models in an attempt to infer the relation between I/O. Essentially, a surrogate model, $\widetilde{\mathcal{M}}_{S_i}$, would be promptly available to map a new state variable $\boldsymbol{x}^{(*)}$ to the strain output of the corresponding sensing location S_i:

$$\widetilde{\mathcal{M}}_{S_i} : \boldsymbol{x}^{(*)} \rightarrow \mathcal{M}_{S_i}^{(*)} \tag{3}$$

In this work GP surrogate models were used as regression algorithms to infer the I/O mappings. The "Regression Learner" of MATLAB's "Statistics and Machine Learning Toolbox" has been utilized to this end. The hyperparameters of the GP models have been estimated via an embodied Bayesian optimization procedure within the toolbox. Cross-validation was achieved via k-fold method. Indicatively, in Figure 4 we present the accuracy among the predicted and the true response of $\widetilde{\mathcal{M}}_{S_1}$ as well as a portion of the surrogate response surface.

3.4 Damage quantification

In the final step, the inverse quantification of the disbond parameters are described. In our methodology, we leverage on the notion that far from damage the strain field remains unaltered [21]; hence, strain readings from sensor R1-R4 are used to infer the load applied on the panel, based on the pristine numerical model. The steps of the damage quantification are presented below:

1. Select reference sensor(s) (R1,..,R4) for load prediction

2. Infer applied load via gradient-descent optimization [21]

3. Infer the deterministic disbond parameters via minimizing the following objective function for a measurement point, m:

$$\{a, d\}^{\top} = \arg\min_{a,d} \left\| \{\widetilde{\mathcal{M}}_{S_i}^{(m)}(a, d \mid P)\}_{i=1}^{N_s} - \{\varepsilon_{S_i}^{(m)}\}_{i=1}^{N_s} \right\|^2 \tag{4}$$

The above expression is minimized via a global optimization algorithm based on radial basis function surrogate models embeddedn within MATLAB.

4 EXPERIMENTAL EVALUATION

4.1 Test campaign

The methodology presented above will be evaluated through a block loading compression-compression fatigue test [19, 25]. More specifically, one SSP containing an artificial skin/stringer disbond via a Teflon-insert is utilized. The nominal area of the disbond is $30\text{x}30$ mm^2 with the central axis of the disbond being located at $a = 210$ mm. The skin panel consists of 14 unidirectional continuum fiber-reinforced with a stacking sequence [45/-45/0/45/90/-45/0]s whereas the stacking sequence of the stringer is [45/-45/0/-45/45]s. The material properties of the plies are presented in Table 1 and of those of the cast-tabs in Table 2.

Table 1: Elastic properties of IM7/8552

Property	Value	Units
Longitudinal Young modulus, E_{11}	161000	MPa
Transverse Young modulus, $E_{22} = E_{33}$	11380	MPa
Poisson ratio, $\nu_{12} = \nu_{13}$	0.32	–
Poisson ratio, ν_{23}	0.45	–
Shear modulus, $G_{12} = G_{13}$	5200	MPa
Shear modulus, G_{23}	3900	MPa

Table 2: Material properties of EPO 5019.

Property	Value	Units
Young modulus, E	6000	MPa
Poisson ratio, ν	0.3	–
Compressive yield strength, S_y^c	110	MPa

The sensorized SSP is presented in Figure 5a. The test plan, as shown in Figure 5b, is defined by discrete fatigue blocks with constant loading ratio, R=10, and frequency f=2 Hz. A quasi-static (QS) test interval is conducted every 500 fatigue cycles, during which, strains are recorded from permanently attached fiber Bragg grating sensors (FBGs), provided by SMARTEC S.A..

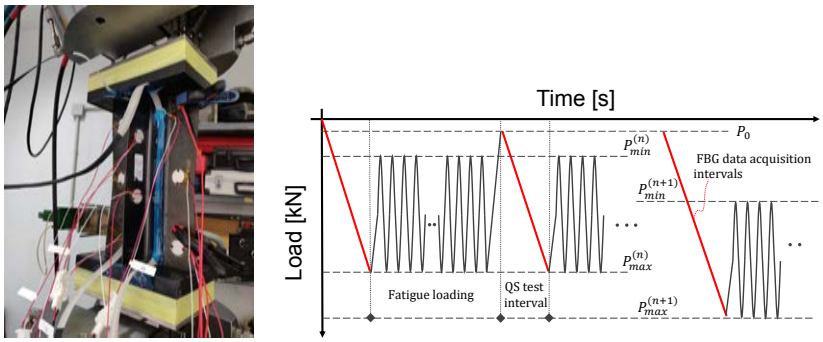

Figure 5: a) The sensorized SSP and b) test plan definition

The FBG readings are used during the online stage to infer the disbond parameters. In this study, only the strains at peak loads are used to asses the methodology. Moreover, in order to evaluate the propagation of the disbonded area as the fatigue progresses, a phased-array ultrasound DolphiCam system was used. In-situ non-destructive evaluation was performed with C-Scan inspections in several occasions while pausing the test. Details about the test characteristics are shown in Table 3.

Table 3: Details of the block loading fatigue test.

Nominal disbonded area $(mm)^2$	P_{min} (kN)	P_{max} (kN)	Total cycles
901.5	-3.5	-35.0	10,000
	-3.9	-39.0	10,000
	-4.5	-45.0	10,000
	-5.0	-50.0	170,000

4.2 Damage quantification results

In this section the disbonded area predictions are being evaluated. In Figure 6a the disbond area predictions are presented associated by groundtruth measurements. From the beginning of the test, the predictions are in accordance with the nominal disbond area, i.e. 901.5 mm^2. Before the maximum load of fatigue was increased to -50 kN, the nominal disbond did not presented propagation evidence. The first evidence of propagation was captured after 80,000 fatigue cycles. The predictions indicated a slight increase of disbonded area until a moment that an abrupt increase was noted, approximately after 80,000 fatigue cycles. After this instance, no significant increase on the disbonded area was observed as can also be indicated by the groundtruth measurements. The deterministic prediction of DT are in a good correlation with the experimental evidence until the final estimation of the area via non-destructive measurement. However, sparse indications of overestimation of the predicted disbonded area may be

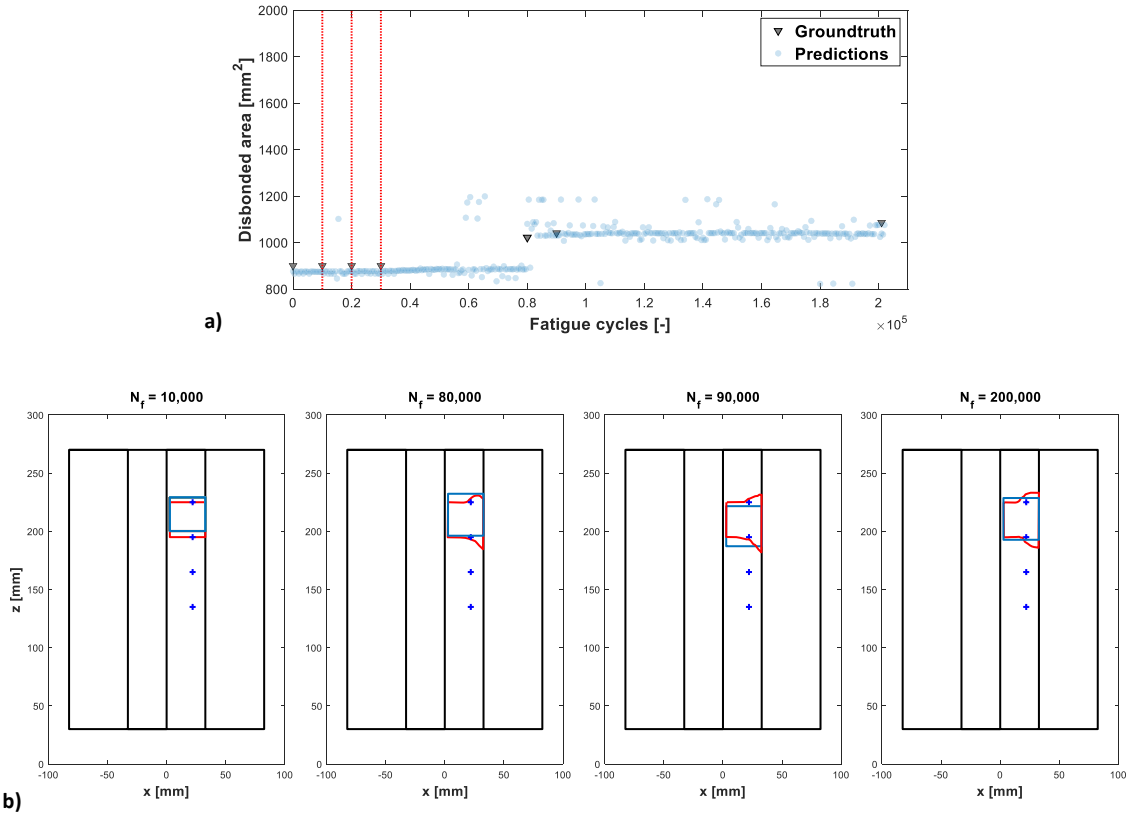

Figure 6: a) Quantification predictions. Vertical red lines indicate moments when the maximum load of fatigue was increased. b) Predicted disbond morphologies (blue shape) versus groundtruth (red shape) as measured after total fatigue cycles applied (N_f)

found, mainly attributed due to the ill-posedness of the inverse problem. This effect may be mitigated by searching the global optimization solution in a judiciously reduced space or applying regularization techniques. In Figure 6b we show the approximation of the disbond morphology with respect to the actual one. It can be also noticed that the methodology is capable of properly estimating the location of the disbond central axis.

5 CONCLUSIONS

In this paper, a numerical campaign of a parametric FE model was employed as data generator to train GP surrogate models. The idea lies in the concept of utilizing the previously trained surrogate models (offline stage) in order to perform disbond quantification predictions for skin/stringer delaminations at composite stiffened panels. A verified FE model produced the damaged strains, at specific sensing locations, which were utilized to effectively train the GP surrogate models. A LH sampling plan has been selected to generate in total 250 discrete rectangle disbonds at various locations and sizes along the longitudinal direction of the panel.

In the end, an inverse approach was followed to estimate the disbond characteristics while the algorithm was fed with real-time experimental strains (online stage). The methodology derives positive predictions regarding the disbonded area as the fatigue test progresses. However, based on the nature of the provided training dataset, the method is limited to estimating a rectangle approximation of the actual disbond morphology, though in a manner that estimates with great accuracy the total disbonded area as well as the location of the central axis.

ACKNOWLEDGMENTS

The author(s) disclosed receipt of the following financial support for the research, authorship, and/or publication of this article: This work was supported by the European Union's Horizon 2020 research and innovation programme MORPHO (Grant Agreement Number: 101006854).

REFERENCES

[1] M. Grieves and J. Vickers, "Digital Twin: Mitigating Unpredictable, Undesirable Emergent Behavior in Complex Systems," in *Transdisciplinary Perspectives on Complex Systems*. Cham: Springer International Publishing, 2017, no. August 2017, pp. 85–113.

[2] D. J. Wagg, K. Worden, R. J. Barthorpe, and P. Gardner, "Digital Twins: State-of-The-Art and Future Directions for Modeling and Simulation in Engineering Dynamics Applications," *ASCE-ASME Journal of Risk and Uncertainty in Engineering Systems, Part B: Mechanical Engineering*, vol. 6, no. 3, 2020.

[3] M. Kapteyn, D. Knezevic, D. Huynh, M. Tran, and K. Willcox, "Data-driven physics-based digital twins via a library of component-based reduced-order models," *International Journal for Numerical Methods in Engineering*, p. nme.6423, jun 2020.

[4] A. Thelen, X. Zhang, O. Fink, Y. Lu, S. Ghosh, B. D. Youn, M. D. Todd, S. Mahadevan, C. Hu, and Z. Hu, "A comprehensive review of digital twin — part 1: modeling and twinning enabling technologies," *Structural and Multidisciplinary Optimization*, vol. 65, no. 12, p. 354, dec 2022.

[5] E. J. Tuegel, A. R. Ingraffea, T. G. Eason, and S. M. Spottswood, "Reengineering Aircraft Structural Life Prediction Using a Digital Twin," *International Journal of Aerospace Engineering*, vol. 2011, pp. 1–14, 2011.

[6] E. H. Glaessgen and D. S. Stargel, "The digital twin paradigm for future NASA and U.S. air force vehicles," *53rd AIAA/ASME/ASCE/AHS/ASC Structures, Structural Dynamics and Materials Conference 2012*, 2012.

[7] J.-A. Pascoe, "Slow-growth damage tolerance for fatigue after impact in FRP composites: Why current research won't get us there," *Theoretical and Applied Fracture Mechanics*, vol. 116, p. 103127, dec 2021.

[8] K. Worden, C. R. Farrar, G. Manson, and G. Park, "The fundamental axioms of structural health monitoring," *Proceedings of the Royal Society A: Mathematical, Physical and Engineering Sciences*, vol. 463, no. 2082, pp. 1639–1664, 2007.

[9] G. Galanopoulos, N. Eleftheroglou, D. Milanoski, A. Broer, D. Zarouchas, and T. Loutas, "An SHM Data-Driven Methodology for the Remaining Useful Life Prognosis of Aeronautical Subcomponents," in *10th European Workshop on Structural Health Monitoring, EWSHM 2022*, 2023, pp. 244–253.

[10] G. Galanopoulos, N. Eleftheroglou, D. Milanoski, A. Broer, D. Zarouchas, and T. Loutas, "A novel strain-based health indicator for the remaining useful life estimation of degrading composite structures," *Composite Structures*, vol. 306, p. 116579, feb 2023.

[11] R. Jin, W. Chen, and T. Simpson, "Comparative studies of metamodelling techniques under multiple modelling criteria," *Structural and Multidisciplinary Optimization*, vol. 23, no. 1, pp. 1–13, dec 2001.

[12] A. Amer and F. Kopsaftopoulos, "Gaussian process regression for active sensing probabilistic structural health monitoring: experimental assessment across multiple damage and loading scenarios," *Structural Health Monitoring*, vol. 22, no. 2, pp. 1105–1139, mar 2023. [Online].

[13] P. E. Leser, J. D. Hochhalter, J. E. Warner, J. A. Newman, W. P. Leser, P. A. Wawrzynek, and F. G. Yuan, "Probabilistic fatigue damage prognosis using surrogate models trained via three-dimensional finite element analysis," *Structural Health Monitoring*, vol. 16, no. 3, pp. 291–308, 2017.

[14] I. N. Giannakeas, Z. Sharif Khodaei, and M. Aliabadi, "Digital clone testing platform for the assessment of SHM systems under uncertainty," *Mechanical Systems and Signal Processing*, vol. 163, p. 108150, 2022.

[15] P. E. Leser, J. E. Warner, W. P. Leser, G. F. Bomarito, J. A. Newman, and J. D. Hochhalter, "A digital twin feasibility study (Part II): Non-deterministic predictions of fatigue life using in-situ diagnostics and prognostics," *Engineering Fracture Mechanics*, vol. 229, p. 106903, apr 2020.

[16] X. Zhou, C. Sbarufatti, M. Giglio, and L. Dong, "A fuzzy-set-based joint distribution adaptation method for regression and its application to online damage quantification for structural digital twin," *Mechanical Systems and Signal Processing*, vol. 191, p. 110164, may 2023.

[17] A. Broer, G. Galanopoulos, R. Benedictus, T. Loutas, and D. Zarouchas, "Fusion-based damage diagnostics for stiffened composite panels," *Structural Health Monitoring*, p. 147592172110071, apr 2021.

[18] N. Yue, A. Broer, W. Briand, M. Rébillat, T. Loutas, and D. Zarouchas, "Assessing stiffness degradation of stiffened composite panels in post-buckling compression-compression fatigue using guided waves," *Composite Structures*, vol. 293, p. 115751, aug 2022.

[19] G. Galanopoulos, D. Milanoski, A. Broer, D. Zarouchas, and T. Loutas, "Health Monitoring of Aerospace Structures Utilizing Novel Health Indicators Extracted from Complex Strain and Acoustic Emission Data," *Sensors*, vol. 21, no. 17, p. 5701, aug 2021.

[20] D. P. Milanoski, G. K. Galanopoulos, and T. H. Loutas, "Digital-Twins of composite aerostructures towards Structural Health Monitoring," in *2021 IEEE 8th International Workshop on Metrology for AeroSpace (MetroAeroSpace)*. IEEE, jun 2021, pp. 613–618.

[21] D. Milanoski, G. Galanopoulos, D. Zarouchas, and T. Loutas, "Multi-level damage diagnosis on stiffened composite panels based on a damage-uninformative digital twin," *Structural Health Monitoring*, vol. 22, no. 2, pp. 1437–1459, mar 2023.

[22] D. P. Milanoski and T. H. Loutas, "Strain-based health indicators for the structural health monitoring of stiffened composite panels," *Journal of Intelligent Material Systems and Structures*, vol. 32, no. 3, pp. 255–266, may 2021.

[23] D. Milanoski, G. Galanopoulos, A. Broer, D. Zarouchas, and T. Loutas, "A Strain-Based Health Indicator for the SHM of Skin-to-Stringer Disbond Growth of Composite Stiffened Panels in Fatigue," in *Proceedings of the 10th European Workshop on Structural Health Monitoring (EWSHM2020)*, vol. 127, 2021, pp. 626–635.

[24] D. Milanoski, G. Galanopoulos, D. Zarouchas, and T. Loutas, "Damage Diagnostics on Post-buckled Stiffened Panels Utilizing the Digital-Twin Concept," in *10th European Workshop on Structural Health Monitoring, EWSHM 2022*, 2023, pp. 213–222.

[25] G. Galanopoulos, D. Milanoski, A. A. R. Broer, D. Zarouchas, and T. Loutas, "Health indicators for diagnostics and prognostics of composite aerospace structures," in *2021 IEEE 8th International Workshop on Metrology for AeroSpace (MetroAeroSpace)*. IEEE, jun 2021, pp. 541–546.